*Astrophysical Masers:*
*Unlocking the Mysteries of the Universe*
*Proceedings IAU Symposium No. 336, 2017*
*A. Tarchi, M.J. Reid & P. Castangia, eds.*

© International Astronomical Union 2018
doi:10.1017/S1743921317010444

# Maser Emission in G 339.884−1.259

**V. Krishnan[1], L. Moscadelli[1], S. P. Ellingsen[2], H. E. Bignall[3], S. L. Breen[4], R. Dodson[5], L. J. Hyland[2], C. J. Phillips[3], C. Reynolds[3] and J. Stevens[3]**

[1]INAF – Osservatorio Astrofisico di Arcetri, [2]University of Tasmania, [3]CSIRO Astronomy and Space Science, [4]University of Sydney, [5]ICRAR University of Western Australia
email: vasaantk@arcetri.astro.it

**Abstract.** We present multi–epoch VLBI observations of the methanol and water masers in the high–mass star formation region G 339.884−1.259, made using the Australian Long Baseline Array (LBA). Our sub–milliarcsecond precision measurements trace the proper motions of individual maser features in the plane of the sky. When combined with the direct line–of–sight radial velocity ($v_{lsr}$), these measure the 3 D gas kinematics of the associated high–mass star formation region, allowing us to probe the dynamical processes to within 1000 AU of the core.

**Keywords.** masers, stars: formation

## 1. Introduction

G 339.884−1.259 is a prominent source in the study of high–mass star formation. It is relatively nearby at a distance of 2.1 kpc (Krishnan *et al.* 2015), shows intense methanol maser emission at 6.7 GHz of ∼1500 Jy — ranking amongst the strongest at this transition — and strong water maser emission of 39.2 Jy at 22 GHz. Many rare methanol maser transitions (e.g. at 19.9, 37.7, 107.0 and 156.6 GHz) have also been found to be coincident with G 339.884−1.259, suggesting that it has an exceptional environment or might be going through a special or short–lived evolutionary phase. These factors contribute to distinguishing it as an interesting source in characterising high–mass star formation.

## 2. Observations

We have conducted VLBI observations of the 6.7 GHz methanol and 22 GHz water masers in G 339.884−1.259 using the Australian Long Baseline Array (LBA). Five epochs of observations of 6.7 GHz masers between 2001 July and 2013 November are used for the analysis presented here. Observations of the water maser emission are from 2016 and 2017. Our aim has been to measure the gas kinematics close to the core(s) from the proper motions of individual maser features over time.

## 3. Proper motions

Figure 1 shows that the distribution of maser emission is perpendicular to the ionised outflow for this source. We identify ten 6.7 GHz methanol maser features which are persistent across three or more continuous epochs for proper motion determination. The proper motions are derived from the procedure in Moscadelli & Goddi (2014) and determined relative to a point which is the mean position of features persistent across all five epochs. The proper motion magnitudes are found to be typically $\lesssim$5 km s$^{-1}$ and primarily in the same direction along the axis of distribution of masers. The exception to this are the features at −39.2, −34.0 and −28.0 km s$^{-1}$. These three largest proper motions are in agreement with the direction of the inferred axis of the ionised outflow from 8.6 GHz radio continuum measurements by Ellingsen, Norris and McCulloch (1996), made using the Australia Telescope Compact Array (ATCA). Interestingly, polarimetric



Downloaded from https://www.cambridge.org/core. IP address: 93.34.136.212, on 26 Oct 2020 at 18:06:37, subject to the Cambridge Core terms of use, available at https://www.cambridge.org/core/terms. https://doi.org/10.1017/S1743921317010444

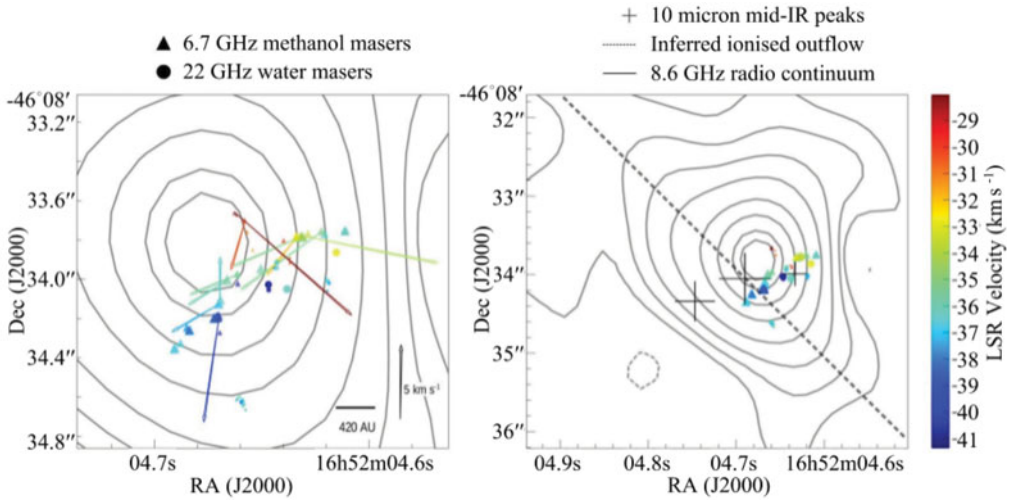



**Figure 1.** Symbol sizes for the maser features and mid–IR peaks are proportional to their flux density. In the left image is a close-up of the proper motions derived from the 6.7 GHz methanol observations. The 22 GHz water maser emission is shown relative to the methanol masers. The image on the right shows the mid–IR and radio continuum emission with respect to the masers. The positional uncertainty is dominated by the $\sim$0.2″ astrometry of the continuum and mid-IR measurements compared to $\sim$5 mas for the masers, which are phase–referenced to a quasar with high positional accuracy. Refer to the electronic copy for a colour version of this figure.

observations by Dodson (2008) show magnetic fields at right angles to the maser distribution, as predicted for a disk model, at the location of the feature at $-39.2$ km s$^{-1}$.

## 4. Fragmentation & evolution in G 339.884−1.259

In Figure 1 (R), we overlay the three 10 $\mu$m mid–IR peaks (1.3, 1.0 and 0.6 mJy) from Keck II observations by De Buizer *et al.* (2002), who argue that the peak of the radio continuum (6.16 mJy beam$^{-1}$) may indicate an additional object. This is therefore a high–mass star formation region with at least four fragmented objects within scales of 2500 AU. Based on the shape of the distribution of the masers and corresponding structure in the mid–IR emission relative to the outflow axis, the sources are in a molecular core elongated along an axis orthogonal to the outflow. There is no detection of 6.7 GHz methanol or 22 GHz water maser emission with the eastern most mid–IR source above a 3$\sigma$ limit of 90 and 120 mJy. As the mid–IR sources are more evolved and less embedded, we speculate that the obscured source associated with the radio continuum peak — in the midst of the maser emission — is at an earlier stage of evolution.

## References

De Buizer, J. M., Walsh, A. J., Piña, R. K., Phillips, C. J., & Telesco, C. M. 2002, *ApJ*, 564, 327

Dodson, R. 2008, *A&A*, 480, 767

Ellingsen, S. P., Norris, R. P. & McCulloch P. M. 1996, *MNRAS*, 279, 101

Krishnan, V., Ellingsen, S. P., Reid, M. J., Brunthaler, A., Sanna, A., McCallum, J., Reynolds, C., Bignall, H. E., Phillips, C. J., Dodson, R., Rioja, M., Caswell, J. L., Chen, X., Dawson, J. R., Fujisawa, K., Goedhart, S., Green, J. A., Hachisuka, K., Honma, M., Menten, K., Shen, Z. Q., Voronkov, M. A., Walsh, A. J., Xu, Y., Zhang, B., & Zheng, X. W. 2015, *ApJ*, 805, 129

Moscadelli, L. & Goddi, C. 2014, *A&A*, 566, A150

Downloaded from https://www.cambridge.org/core. IP address: 93.34.136.212, on 26 Oct 2020 at 18:06:37, subject to the Cambridge Core terms of use, available at https://www.cambridge.org/core/terms. https://doi.org/10.1017/S1743921317010444